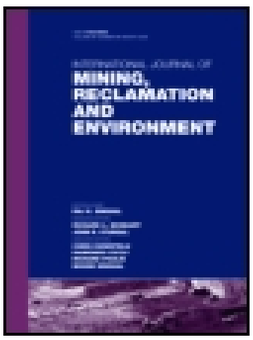

International Journal of Surface Mining, Reclamation and Environment

ISSN: 1389-5265 (Print) 1744-5000 (Online) Journal homepage: https://www.tandfonline.com/loi/nsme19

Influence of blast delay time on rock fragmentation: One-tenth scale tests

Mark S. Stagg

To cite this article: Mark S. Stagg (1987) Influence of blast delay time on rock fragmentation: One-tenth scale tests, International Journal of Surface Mining, Reclamation and Environment, 1:4, 215-222, DOI: 10.1080/09208118708944122

To link to this article: https://doi.org/10.1080/09208118708944122

Influence of blast delay time on rock fragmentation: One-tenth scale tests

Mark S.Stagg
US Department of the Interior, Twin Cities Research Center, Bureau of Mines, 5629 Minehaha Avenue, South, Minneapolis, Minnesota 55417, USA

1 ABSTRACT

The Bureau of Mines is studying blast delay timing influences on rock fragmentation in a series of tests that started in 3-ft concrete blocks and includes reduced-scale and full-scale bench blasts. This paper reports on the reduced-scale tests. In a 45-in high dolomite bench, 18 single-row blasts were fired with 15-in burdens. Spacings were 21 and 30 in. Delay intervals ranged from 0 to 45 ms, equivalent to 0 to 36 ms/ft of burden. Each shot was instrumented for strain and pressure for both in situ dynamics and interactions between blastholes. All fragmented rock was screened.

The finest fragmentation occurred at blasthole delay intervals of 1 to 17 ms/ft of burden. In this range, stress-wave-induced strains interacted with longer lasting gas-pressure strains from earlier holes. Coarse fragmentation resulted from short delays (<1 ms/ft), where breakage approached presplit conditions with a major fracture between blastholes and large blocks in the burden region. Coarse fragmentation also resulted from long delays (>17 ms/ft), with explosive charges acting independently. The broad acceptable range provides blast design tools useful for a variety of purposes, including optimum muckpile displacement and vibration control.

2 INTRODUCTION

The explosives industry is developing and testing delay blasting caps of improved accuracy. Precise delays have been cited as factors in controlling blast vibration amplitude and frequency and improving fragmentation (Chiappetta, 1986 - Reil, 1985). However, data on complete fragmentation assessment of shots initiated with precise days is limited. As part of its blasting research program, the Bureau of Mines is examining the influence of timing intervals by completely screening the blast-induced rock. Three- and four-hole shots have been conducted in concrete blocks in the laboratory and at reduced (45-in bench) and full (22-ft bench) scale in the field. Tests thus far have mostly been concerned with the effect of delay time on fragmentation and on the interaction between shotholes. Initial testing in the laboratory provided an effective means for establishing a methodology of controlled experimentation. The tests at reduced scale in the field provided experience in fragmentation assessment techniques and results that could be used to optimize the expensive full-scale field tests. The full-scale field tests are currently in progress. This paper discusses the reduced-scale field tests and results.

The reduced-scale field tests were conducted at the University of Missouri's Experimental Mine in Rolla. This site was chosen because of its accessibility and geology, and the cooperation available from the University. Furthermore, the results of previous research conducted at the mine on blast design and fragmentation were reported in several theses (Bleakney, 1982, Brinkman, 1982, Smith, 1976). These studies investigated various design factors affecting fragmentation, such as coupling, initiation sequence, primer location, and airgap, and provided a comparison with the Bureau test results.

3 SITE

The experiment was conducted in a 45-in bench of dolomite, part of the Jefferson City Formation. The rock is of irregular grain size, 10 pct calcite, and thick bedded with a specific gravity of 2.65 and compressional and shear velocities of 14,800 and 8,100 ft/s, respectively (Smith, 1976). Bureau researchers verified these values by in situ seismic measurements behind the blastholes, finding 14,700 ft/s (compressional) and 8,100 ft/s (shear).

The reduced-scale tests were designed to be geometrically proportional to typical full-scale bench blasts with dimensions about 10 pct of full scale. However, at reduced scale, rock structures such as bedding and jointing are exaggerated and can have an unrealistic effect. The massive dolomite at the Rolla site provided a good medium for the reduced-scale testing since only three bedding planes were in the 45-in bench and no jointing was observed within any of the test shots.

4 PROCEDURES

In order to prepare the pit and bench for the tests, development work was necessary to provide consistent geometry of the working faces. Horizontal holes were drilled 45 in above the pit floor to give the proper bench height, and vertical holes were drilled to obtain a vertical face. For each test shot, an open end at an angle of approximately 135° was formed, as shown in figure 1. To form the single-row pattern, three shotholes were drilled to 50-in depth, including 5 in of subdrill. The burden was held constant at 15 in, and spacings were 21 and 30 in, spacing-to-burden ratios (S/B) of 1.4 and 2.0, respectively. All faces were cleaned with a scaling bar and blown with air to remove loose material, and the entire area swept clean prior to each shot.

Each hole contained 144 g of 60 pct extra-high-density dynamite tamped into a 1/2-in-(ID) plastic tube 40-in long. Each charge was bottom-primed and initiated by an exploding bridgewire detonator

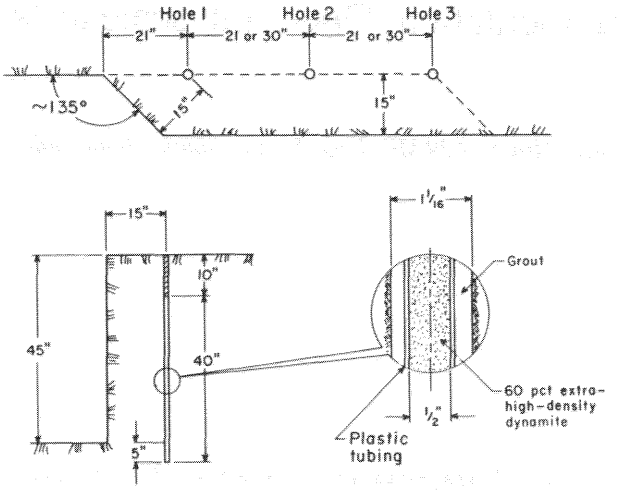

Figure 1. Shot pattern and blast design for reduce-scale tests.

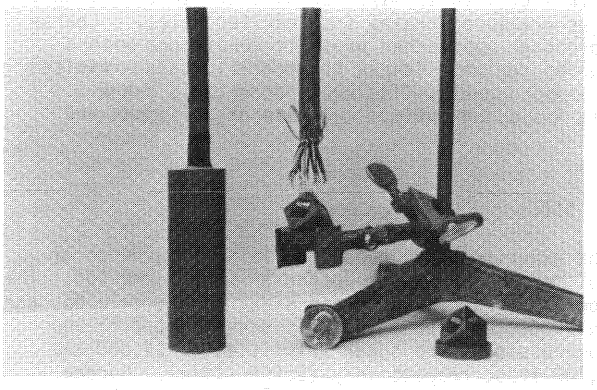

Figure 2. Stages of assembly of six-component strain gauge.

(EBW). Complete coupling was assured by placing the charge into grout-filled holes. The initiation system for the EBW's consisted of a power supply, firing module, and digital delay generator with a firing accuracy of 0.0025 pct times the delay time or ± 50 ns, whichever is greater.

Most shots were instrumented with dynamic-strain and pressure gauges (figs. 2-3). The strain gauges were a six-component type, built after a design by Reed (Reed, 1979) as modified by Anderson (Anderson, 1979). These gauges were grouted into the burden region at various locations between the boreholes. Pressure gauges were placed either above the strain gauges or in inclined holes in the face, which were filled with a water-revert mixture. The pressure gauges were of two types, carbon resistors dipped in liquid tape (insulating coating) and Navy-built tourmaline gauges in an oil-filled boot. Also, a fiber optic system was used to measure detonation velocities. Data were recorded on a 28-channel Wide Band I (80 kHz) recorder and a digital oscilloscope, with a 0.5 μs response rate.

To contain flyrock and minimize secondary breakage, the entire shot was covered with a blasting mat held in place with timbers and anchoring cables (fig. 4). The area in front of the shots was covered with a plastic sheet to aid in identifying blasted material. Flyrock went beyond the sheeting for only a few shots. This rock was identified when possible and included with the muckpile.

Screening of the muckpile began immediately after

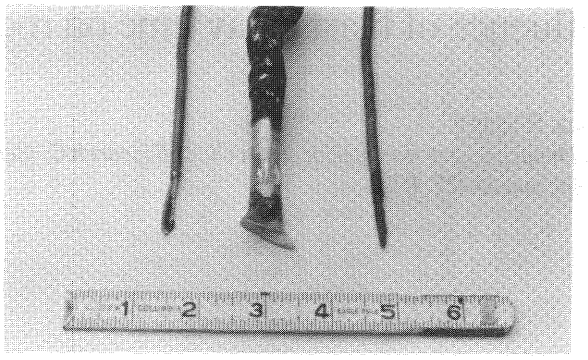

Figure 3. Carbon resistor (left and right) and tourmaline (center) pressure gauges.

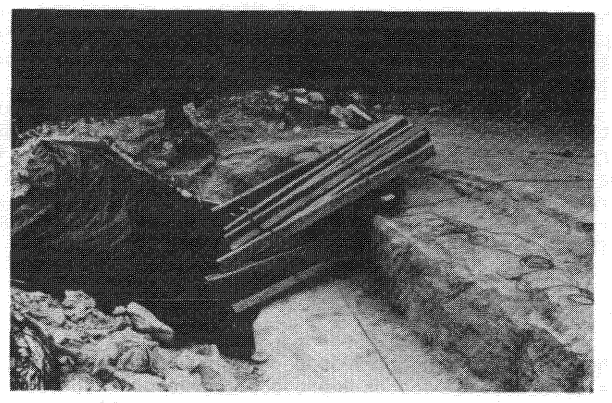

Figure 4. Pit area with blasting mat and timbers covering test shot.

each shot. All fragments 3 in and larger were sized and weighed in the pit. The pit size fractions were minus 3, plus 3, minus 6, plus 6, minus 12, and plus 12 in. Material passing the 3-in screen was loaded into containers, removed from the pit, and mechanically shaken through screens. These size fractions were plus 1-1/2 minus 3, plus 3/4 minus 1-1/2, plus 3/8 minus 3/4, plus 3/16 minus 3/8, and minus 3/16 in. From the weight of each fraction, its percentage of the total muckpile was calculated.

5 ANALYSIS AND RESULTS

A total of 24 blasts were detonated. Two were development shots. Of the remainder, nine at 21-in spacing and nine at 30-in spacing were completely screened, three misfired, and one was a single-hole test shot. Delay intervals ranged from simultaneous to 36.0 (ms/ft) of burden. Table 1 lists the reduced-scale (RS) shots.

Since these tests were designed to determine the effect of delay time on fragmentation, i.e., the interaction between shotholes, it was decided to identify any overbreak from each shot and to size and weigh it separately from the muckpile. A third of the shots produced no back or end-overbreak. There was no obvious correlation between spacing or timing and those shots producing overbreak, which was generally oversized and averaged 10 pct of the total blasted rock weight. Because the overbreak skewed the particle size distributions at the high end and came from outside the shot pattern, it was removed from the corresponding size fraction and not included in the analysis of fragmentation. Table 2 lists the sieve weights for the shots.

Table 1. Reduced-scale (RS) test shots

Shot[1]	Spacing, inch	Delay time: Between holes, ms	Delay time: ms/ft of burden	Shot[1]	Spacing, inch	Delay time: Between holes, ms	Delay time: ms/ft of burden
RS-3....	30	20.0	16.0	RS-14...	30	1.25	1.0
RS-4....	30	7.5	6.0	RS-15...	30	0	0
RS-5....	30	5.0	4.0	RS-16...	30	45.0	36.0
RS-6....	30	20.0	16.0	RS-17...	30	2.5	2.0
RS-9....	21	0	0	RS-18...	21	21.0	16.8
RS-10...	21	30.0	24.0	RS-19...	21	1.75	1.4
RS-11...	21	14.0	11.2	RS-21...	21	.4375	.35
RS-12...	21	3.5	2.8	RS-22...	21	8.75	7.0
RS-13...	30	30.0	24.0	RS-23[2]..	NA	NA	NA
				RS-24...	21	45.0	36.0

NA Not applicable. [1]Not listed: Shots RS-1 and RS-2 (development shots) and RS-7, RS-8, and RS-20 (misfires). [2]Single-hole shot.

Table 2. - Weight of rock fragments at various screen sizes, pounds

Shot	Screen size, in: -3/16	+3/16 -3/8	+3/8 -3/4	+3/4 -1-1/2	+1-1/2 -3	+3 -6	+ 6 -12	+12 -24
RS-3...	208	243	268	535	639	1,389	1,607	241
RS-4...	172	243	263	570	675	1,987	2,022	241
RS-5...	215	237	258	498	523	1,628	1,941	159
RS-6...	188	216	257	466	596	1,656	1,745	117
RS-9...	196	182	196	356	421	1,197	1,173	1,415
RS-10..	232	259	320	552	631	1,372	2,100	172
RS-11..	305	318	391	587	572	1,149	800	0
RS-12..	233	255	298	557	639	1,521	1,147	0
RS-13..	238	238	276	452	516	1,550	1,857	520
RS-14..	217	240	253	541	612	1,911	1,718	266
RS-15..	167	182	208	466	521	1,657	2,092	462
RS-16..	244	250	246	471	512	1,607	2,019	536
RS-17..	242	247	309	522	630	1,801	1,546	446
RS-18..	246	275	342	522	590	1,197	876	0
RS-19..	202	234	302	548	635	1,219	911	0
RS-21..	203	194	198	377	449	1,132	1,507	688
RS-22..	268	235	258	454	501	1,131	1,022	143
RS-23..	71	60	61	123	138	364	550	178
RS-24..	295	249	270	486	541	1,060	1,110	422

The cumulative percent passing versus sieve size is plotted in figure 5 for four shots at each spacing, covering the range of delay times tested. The material that passed through the 24-in sieve would in most cases have passed through a much smaller sieve, even down to 13 in. Since the largest size piece was not measured and 24 in is too large, the 24-in point has been omitted from the curves, except that it was used to obtain the 80-pct-passing value for shot RS-9, as shown in figure 5. The curves in figure 5 are representative of the results, which showed a dramatic improvement, a 20- to 50- pct reduction in average size, occurred at delays of ~1.0 to 17.0 ms/ft compared with simultaneous initiation. At delays longer than 17.0 ms/ft, the average size increased ~20 to 50 pct.

The 20-, 50-, and 80-pct-passing sizes versus delay period, shown in figure 6, were determined for all the tests from percent-passing curves similar to those shown in figure 5. The delay period had little effect on the size of fragments in the 20-pct-passing fraction, except that they were slightly coarser at the simultaneous shots. At both spacings, the 50- and 80-pct-passing fractions show that delays of 1 to 17 ms/ft produced the finest fragmentation. Poorest or coarsest fragmentation was observed for simultaneous shots and for shots with delay intervals >24 ms/ft, although the differences at the longer delays were smaller with the 30-in spacings. The improved fragmentation obtained for most of the shots at 21-in spacings, as compared with 30-in spacings, was expected and was due in part to a higher powder factor. However, the coarsest fragmentation resulted at the very short delay times for the 21-in spacing tests even though there was a higher powder factor.

To quantify the test results and ultimately develop an equation to predict fragmentation, it is necessary to develop a mathematical description of the cumulative percent-passing data. Previous researchers have used regression analysis to fit observed blast fragmentatation data to logarithmic, power (Da Gama, 1983), Gaussian (Reil, 1985), and Weibull distributions (Cunningham, 1983, Hjelmberg, 1983). Analysis-of-variance tests can then be used to determine the statistical significance of the effect of delay time on the cumulative size distribution functions. These tests determine whether a single regression line can be used to represent the combined results of several shots. If pooling or combining the results tests positive, then there exists a statistical inference that the delay time has not significantly affected fragmentation.

Statistical tests were run on several regression line fits to the data, and the correlation coefficients (R) for the various distributions are given in table 3. The data shown in figure 6 suggest that the finer size material was less affected by delay time. An examination of the weights of the material passing the 3-in sieve found minimal variability, as shown in figure 7, except for shots at delays less than 1.0 ms/ft. Excluding these shots and an extremely high (2,170 lb) outlier value, the weight of material passing the 3-in sieve

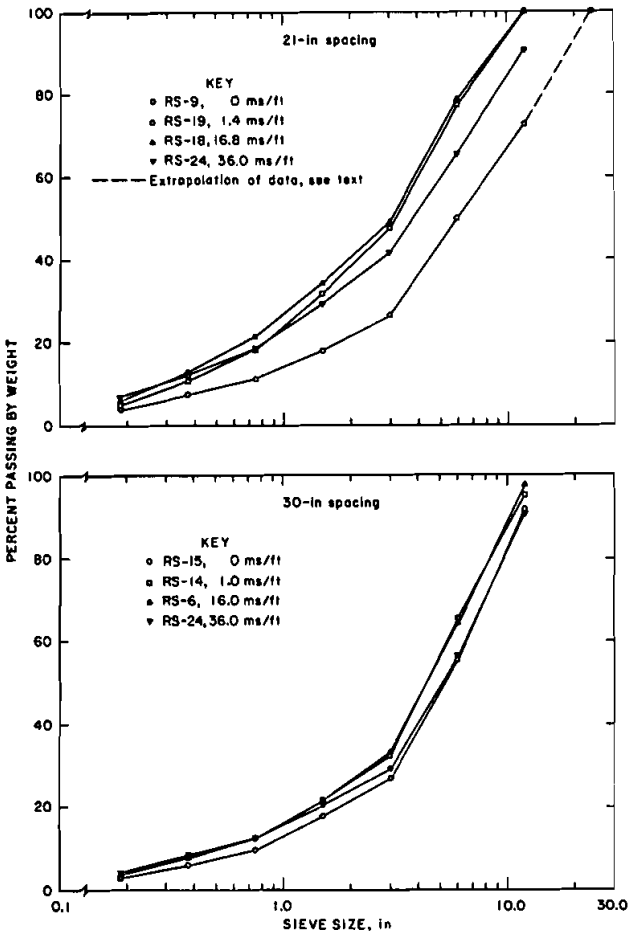

Figure 5. Particle size distribution for shots at 21- and 30-in spacings.

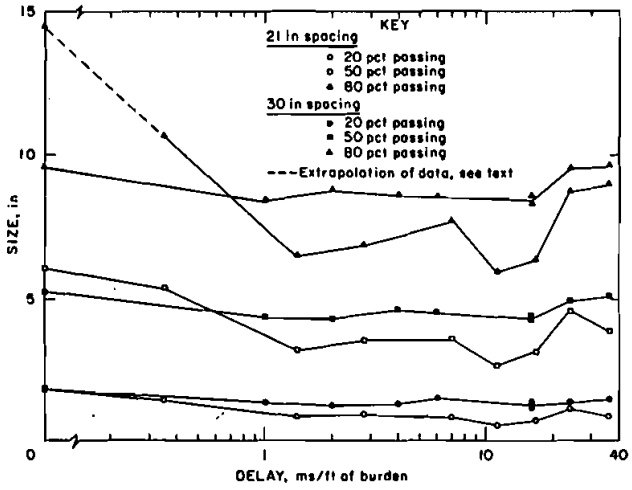

Figure 6. Size at 20-, 50-, and 80-pct passing versus delay period for shots at 21- and 30-in spacings.

ranged from 1,716 to 1,994 lb and 1,720 to 1,950 for the 21- and 30-in-spacing shots, respectively. The nearly constant weight of finer material suggests that a fractured zone extends around the borehole, which, assuming a cylindrical nature, would have a radius of 10 in. This equates to 40 explosive radii, within the range of the damage zone predicted by Siskind (Siskind, 1973, Siskind, 1974), Olson

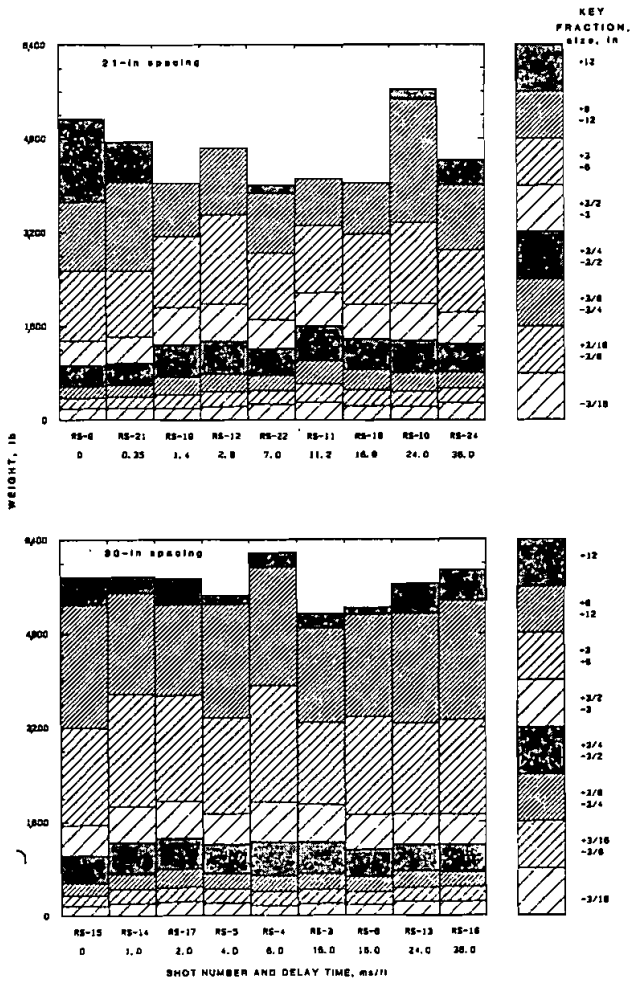

Figure 7. Weight retained on each size fraction for shots at 21-and 30-in spacings.

Table 3. Correlation coefficients for Weibull, power and Gaussian distributions

Shot	Weibull		Power		Gaussian
	A[1]	B[2]	A[1]	B[2]	B[2]
RS-3...	0.9923	0.9861	0.9963	0.9980	0.9999
RS-4...	.9906	.9858	.9961	.9944	.9995
RS-5...	.9833	.9758	.9972	.9941	.9993
RS-6...	.9856	.9815	.9874	.9953	.9998
RS-9...	.9961	.9936	.9978	.9942	.9837
RS-10..	.9859	.9720	.9966	.9980	.9979
RS-11..	.9966	.9852	.9876	.9956	.9996
RS-12..	.9958	.9845	.9948	.9941	.9992
RS-13..	.9893	.9847	.9973	.9946	.9988
RS-14..	.9893	.9868	.9972	.9923	.9981
RS-15..	.9895	.9848	.9982	.9948	.9993
RS-16..	.9872	.9830	.9971	.9940	.9992
RS-17..	.9832	.9906	.9970	.9928	.9945
RS-18..	.9966	.9875	.9902	.9933	.9998
RS-19..	.9978	.9909	.9913	.9932	1.0000
RS-21..	.9921	.9887	.9981	.9970	.9980
RS-22..	.9904	.9862	.9966	.9957	.9994
RS-24..	.9956	.9921	.9968	.9980	.9964

[1]All data points used in regression analysis except the +12-, 24-in data point. [2]Only data at 1-1/2-, 3-, 6-, and 12-in sizes used; 100-pct point also excluded.

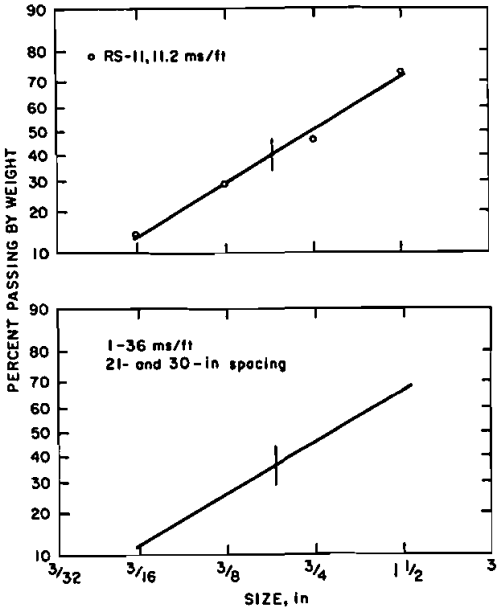

Figure 8. Log-normal distribution for material passing 1-1/2-in sieve size.

(Olson, 1973), and others in terms of charge radii (i.e., 20 to 40 radii). As shown in figure 8, the fines best fit a log-normal distribution. Analysis-of-variance tests were run for all finer-size data from delays of 1 to 36 ms/ft, and one curve could be used to represent the data at both spacings. For shots at delays less than 1 ms/ft, the weight of fines was reduced.

The correlation coefficients in table 3 show that a Gaussian distribution for the coarser site data usually produced the best fit. The Gaussian, power and Weibull fits to the coarse size data are shown in figure 9 for shots RS-3 and RS-13. It was observed that the 1-1/2-in sieve material also fit the Gaussian distribution, and this material was included in the regression analysis of table 3. The coarse material is assumed to be generated primarily between the boreholes outside the extended fractured zone that exists around the borehole.

An attempt to pool all of the data using a Gaussian distribution indicated (at a 95-pct-confidence level) that the delay time was indeed significant. Further analysis-of-variance tests were conducted to see if certain shots could be pooled to form one regression line. For example, the 21-in shots at 11.2 and 16.8 ms/ft could be combined (i.e., there was no effect due to delay time). The 30-in shots at 1, 2, 4 and 6 ms/ft could also be combined. Figure 10 is a plot of the 50- and 80-pct-passing value determined from the Gaussian distributions. A horizontal line is drawn for delays that could be pooled into one regression line.

Although not shown in the figure, the single-hole fragmentation distribution pooled with the 30-in spacing curves at delays of 24 and 36 ms/ft. Apparently, firing holes at delays of >24 ms/ft can be considered as firing single-hole shots. It is noteworthy that the distance from the corner to the first hole was 21 in (fig. 1), but the fragmentation data pooled with the 30-in spacing tests. The single-hole test reflected the 30-in results because at 21-in, the first hole's breakout angle, >135°, reduced the burden distance for subsequent holes, which improved fragmentation over that resulting from single-hole shot.

The 50- and 80-pct curves of figures 6 and 10 are quite similar except for the simultaneous shot at 21-in spacing, RS-9. The Gaussian distribution was

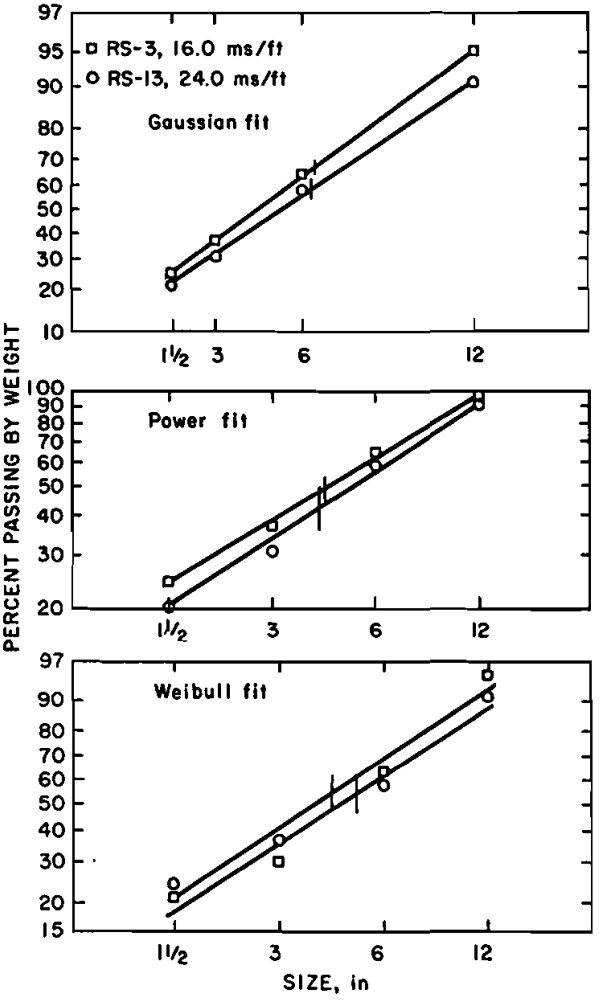

Figure 9. Comparison of Gaussian, power, and Wiebull distributions.

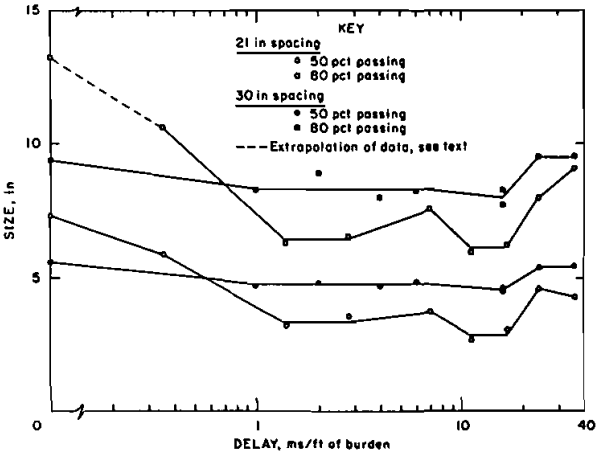

Figure 10. Size at 50-and 80-pct-passing versus delay period from Gaussian distribution fits to the 21-and 30-in spacing data.

not the best fit for this shot, and the regression line predicts a higher value than the data suggest.

As mentioned earlier, the University of Missouri's Experimental Mine has been used by several researchers (Bleakney, 1982, Brinkman, 1982, Smith, 1976) to conduct investigations of blast design and fragmentation. Where possible, these data have been

compared with Bureau results, as shown in figure 11. Since the shot designs for these tests were similar by those used by the Bureau, the fragmentation results compare very favorably. Other research, such as Bergmann's multi-hole tests in granite blocks (Bergmann, 1974), showed a similar significant improvement in fragmentation as delay times increased from simultaneous to 1 ms/ft of burden. Winzer's tests in limestone blocks and in a small bench (Winzer, 1983) resulted in a relationship between delay time and fragmentation that correlates well with Bureau results. The character of the data in figure 11 is similar, showing substantial improvement in fragmentation as delays increase to 1 ms/ft, slightly coarser fragmentation between 6 and 7 ms/ft, and continued improvement to 10 ms/ft.

Strain and pressure records obtained for the reduced-scale tests tend to confirm the fracture development mechanisms observed and reported by Holloway in work done under contract to the Bureau (S0245046, 1986). Initially, a fracture zone develops around the borehole because of the development of radial fractures and fracturing caused by reflected stress waves. The radial fractures propagate at speeds down to 12 pct of the P-wave velocity (Holloway, 1980). The fractured region for these tests appeared to coincide with the finer material zone, which was generated within about 40 charge radii. From pressure gauges installed in this zone, the velocity of explosive gases penetrating fractures was found to be approximately 1,800 to 2,700 ft/s, as shown in figure 12. The large impulsive signals on the records were due to the pickup of electrical noise from the EBW initiation system and were used to confirm the delay intervals.

The P-wave velocities were determined from the arrival times and the distances from shotholes to gauges. The distance and arrival time measurements used to calculate the velocity of gas movement through the rock were adjusted to correct for the travel time of the bottom initiated explosive detonation (8,000 ft/s) to the height of the gauge.

The borehole pressure and radial crack pressurization produce stresses in the material beyond the near fracture zone, and this leads to additional failure and extension of the radial cracks to the free face. The velocity of gas penetrating fractures was estimated to be 146 ft/s for shot RS-14, as shown in figure 13. This velocity was determined by subtracting from the arrival time the travel time of the explosive to the gauge height and the time of gas penetration (1,800 ft/s) out to 10 in. The remaining distance to the

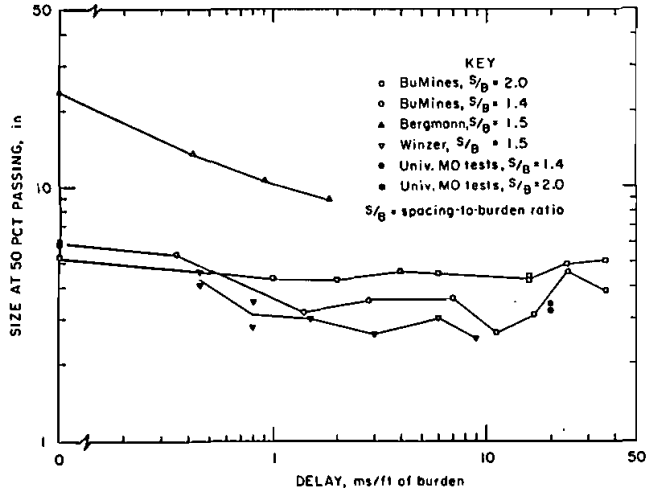

Figure 11. Comparison of reduced-scale data with results obtained by other researchers.

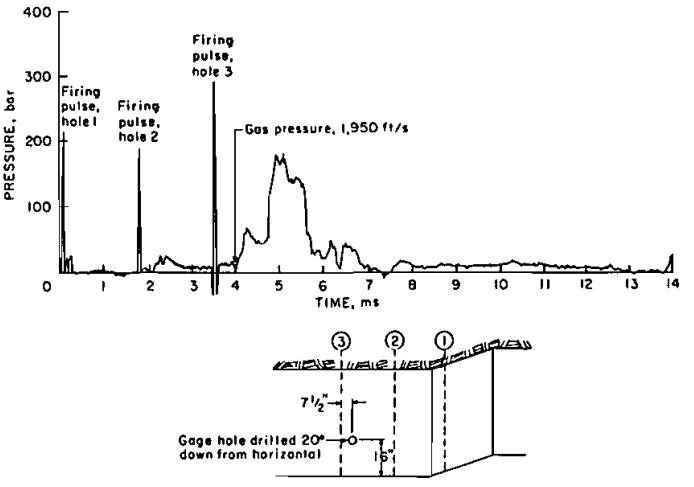

Figure 12. Pressure measured for shot RS-19.

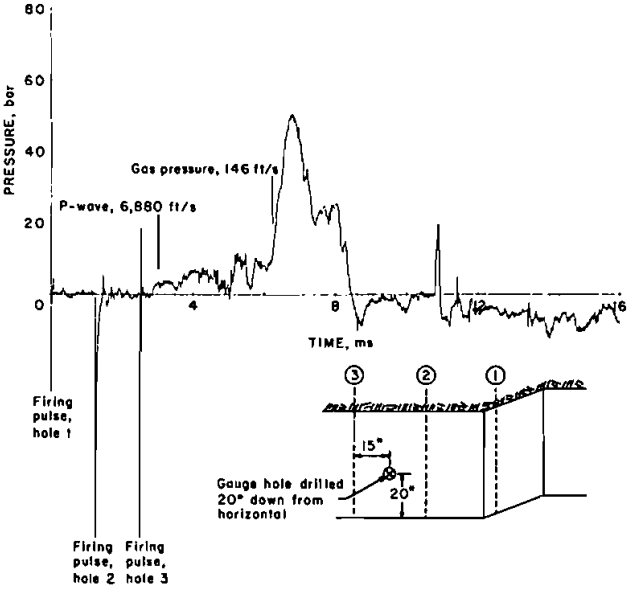

Figure 13. Pressure measured for shot RS-14.

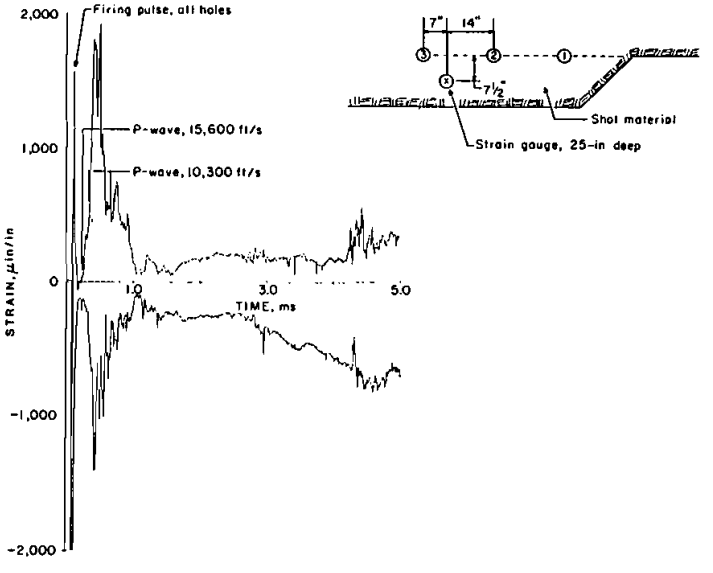

Figure 14. Principal strains measured for shot RS-9.

gauge and the remaining time were used to determine the velocity.

Strain data from the shots were processed into resultant principal strains, octahedral shear strain and dilatation (Anderson, 1984). Two of the principal strains are plotted in figures 14 through 17 for test shots with simultaneous and 1.4-, 2.0-, and 16.0-ms/ft delays. Shown on the records are the calculated P-wave and gas velocities determined from arrival times and shothole to gauge distances as discussed earlier. The strain pulses increased in amplitude with decreasing distances from shothole to gauge. These pulses correspond to the arrival of stress waves, which often arrived increasingly later in time as holes 2 and 3 were fired. The observed decrease in compressional (P) and shear (S) velocities is probably due to flaws in the rock, such as fractures and cracks produced by stress waves from an earlier shothole.

The gas velocities observed on the strain records agreed with pressure gauge gas velocity observations, except for those in shot RS-2, where it is believed a major crack developed in line with holes 2 and 3, causing the observed gas velocity of ~2,000 ft/s. Excessive end-break was noted for this development shot.

Optimum fragmentation occurred when a hole fired such that its stress wave interacted with the stress induced by the expanding gas pressurization from the previous hole. Shots RS-2 and RS-6 show a long-term strain believed to be induced by the late-arriving gas pressure interacting with the stress wave from hole 3. Similar measurements and observations have been made at full scale (Reil, 1985). The interactions of strains induced by the stress waves and strains induced by gas pressure was not always observed for all shots of optimum delay (1 to 17 ms/ft), because the gauge is stressed only if near a pressurized crack and well-coupled to the rock. These interactions were also not observed for shots with delay times outside the optimum range. Even though shot RS-19, shown in figure 15, does not show an interaction at the gauge location, pressure effects are still observed later in the record. Gas effects are not as apparent for the simultaneous shot, shown in figure 14.

Fragmentation results at short delays (less than 1 ms/ft of burden) suggest that fracturing in the zone around the borehole must be completed before the next hole fires. Using 1,800 ft/s as the velocity for crack development in the 10-in zone around the borehole, plus the explosive detonation time (.42 ms), the next hole should not be fired until after

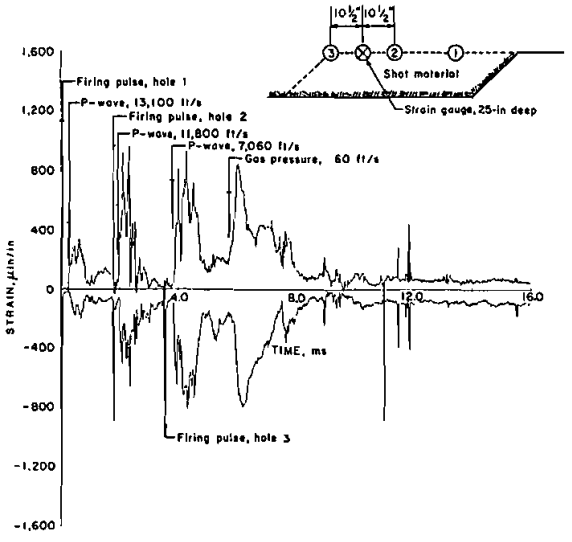

Figure 15. Principal strains measured for shot RS-16.

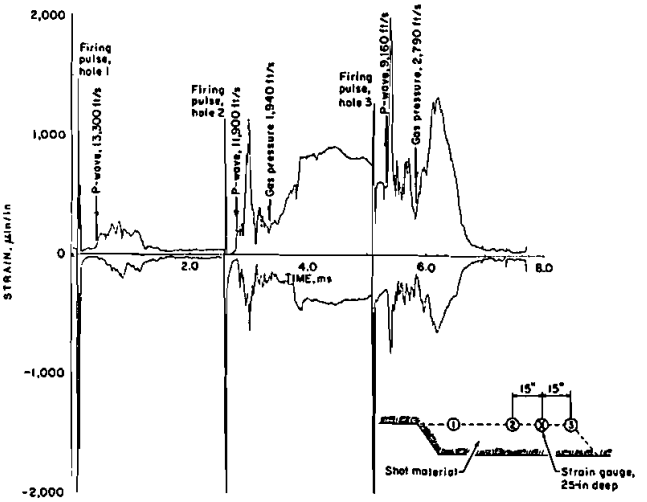

Figure 16. Principal strains measured for shot RS-2.

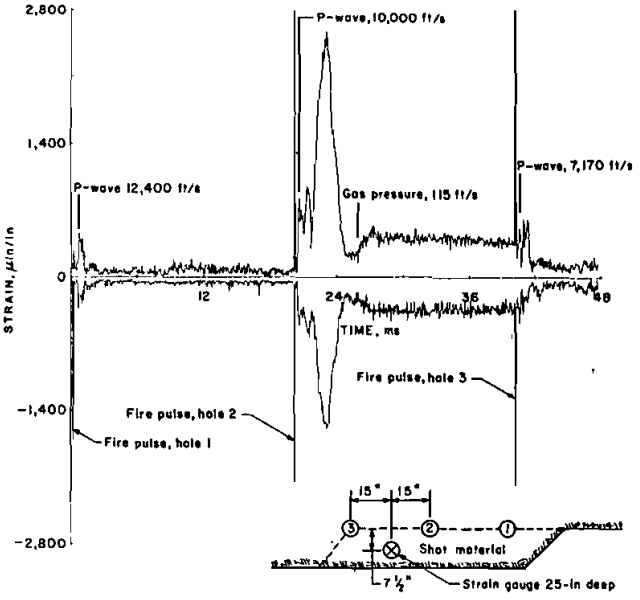

Figure 17. Principal strains measured for shot RS-6.

0.9 ms or 0.7 ms/ft. Enhanced cracking appears to last as long as the gas is retained. Gas velocities through the rock suggest the process will last up to 20 ms or 16 ms/ft, based on a 45° breakout angle and gas penetration velocities of 1,800 ft/s for the first 10 in and 50 ft/s for the next 11 in.

6 CONCLUSIONS

An investigation of the effect of delay time on fragmentation was conducted at a reduced scale using three blastholes per shot in a 45-in bench. With the burden constant at 15 in, delay intervals were varied from 0.0 (simultaneous) to 36.0 ms/ft of burden, and the entire muckpile was screened to assess fragmentation for tests with 21- and 30-in blasthole spacings.

Attempts were made to mathematically describe the distribution of fragment sizes using power and Weibull functions, which have been used by other researchers. However, regression analysis indicated the Bureau data were best described by a Gaussian or

simple normal distribution. Materials excluded from the analysis were overbreak, which came from outside the shot area, and fines, which were determined to come from the immediate blasthole vicinity and showed little variability from shot to shot.

Analysis-of-variance tests showed that delay time did influence the distribution of fragment sizes for both spacings, but more so for the 21-in spacing. Fragmentation was coarsest for shots fired simultaneously and at delay times of 24 ms/ft of burden and greater. Better fragmentation was observed for delay times from 1 to 17 ms/ft, with the tests at 11.2 and 16.8 ms/ft resulting in the best fragmentation. Dynamic strain and pressure measurements indicated that this improved fragmentation may be the result of strains induced by stress waves constructively interacting with strains induced by gas pressure from an earlier detonated hole.

7 REFERENCES

Chiappetta, R. F., S. L. Burchell, D. A. Anderson, and J. W. Reil. Effect of Precise Delay Times on Blasting Productivity, Ground Vibrations, Airblast, Energy Consumption and Oversize. Paper in Proceedings of the 12th Annual Conference on Explosives and Blasting Technique, ed. by C. J. Konya (Atlanta, GA, Feb. 1986). Soc. Explos. Eng., Montville, OH, 1986, pp. 213-240.

Reil, J. W., D. A. Anderson, A. P. Ritter, D. A. Clark, S. R. Winzer, and A. J. Petro. Geologic Factors Affecting Vibration From Surface Mine Blasting (contract HO222009, Vibra-Tech Eng., Inc.). BuMines OFR 33-86, 1985, 204 pp,; NTIS PB 86-175858.

Bleakney, E. L. A Study of Fragmentation and Ground Vibration With Air Space in the Blasthole. M.S. Thesis, Univ. MO-Rolla, 1982, 83 pp.

Brinkman, J. R. The Influence of Explosive Primer Location on Fragmentation and Ground Vibrations for Bench Blasts in Dolomitic Rock. M. S. Thesis, Univ. MO-Rolla, 1982, 83 pp.

Smith, N. S. Burden Rock Stiffness and Its Effect on Fragmentation in Bench Blasting. Ph.D. Thesis, Univ. MO-Rolla, 1976, 148 pp.

Reed, R. P. Triaxial Measurement of Stress Waves in the Free-Field. Sandia Lab., Albuquerque, NM, Rep. SAND-78-212236, 1979, 21 pp.

Anderson, D. A., S. R. Winzer, and A. P. Ritter. Time-Histories of Principal Strains Generated in Rock by Cylindrical Explosive Charges. Paper in Rock Mechanics in Productivity and Protection, ed. by C. H. Dowding and M. M. Singh (Proc. 25th U.S. Symp. on Rock Mechanics, Evanston, IL, June 25-27, 1984). Soc. Min. Eng. AIME, 1984, pp. 959-968.

Da Gama, D. Use of Comminution Theory to Predict Fragmentation of Jointed Rock Masses Subjected to Blasting. Paper in First International Symposium on Rock Fragmentation by Blasting. Lulea Univ. Technol., Lulea, Sweden, 1983, pp. 565-579.

Cunningham, C. The Kuz-Ram Model for Prediction of Fragmentation From Blasting. Paper in First International Symposium on Rock Fragmentation by Blasting. Lulea Univ. Technol., Lulea, Sweden, 1983, pp. 439-453.

Hjelmberg, H. Some Ideas on How to Improve Calculations of the Fragment Size Distribution in Bench Blasting. Paper in First International Symposium on Rock Fragmentation by Blasting. Lulea Univ. Technol., Lulea, Sweden, 1983, pp. 469-494.

Siskind, D. E., R. C. Steckley, and J. J. Olson. Fracturing in the Zone Around a Blasthole, White Pine, Mich. BuMines RI 7753, 1973, 20 pp.

Siskind, D. E. and R. R. Fumanti. Blast-Produced Fractures in Lithonia Granite. BuMines RI 7901, 1974, 38 pp.

Olson, J. J., R. J. Willard, D. E. Fogelson, and K. E. Hjelmstad. Rock Damage From Small Charge Blasting in Granite. BuMines RI 7751, 1973, 44 pp.

Bergmann, O. R., F. C. Wu, and J. W. Edl. Model Rock Blasting Measures Effect of Delays and Hole Patterns on Rock Fragmentation. Eng. and Min. J., v. 175, June, 1974, pp. 124-127.

Winzer, S. R., D. A. Anderson, and A. P. Ritter. Rock Fragmentation by Explosives. Paper in First International Symposium on Rock Fragmentation by Blasting. Lulea Univ. Technol., Lulea, Sweden, 1983, pp. 225-249.

Holloway, D. C., D. B. Barker, and W. L. Fourney. Dynamic Crack Propagation in Rock Plates. Paper in the State of the Art in Rock Mechanics (Proc. 21st U.S. Symp. on Rock Mechanics, Rolla, MO., May 28-30, 1980): Univ. MO-Rolla, 1980, pp. 371-379.